HOS-86-01

Ultimate Soil Resistance of "Chance" Anchors and Concrete Footings for Horizontal Loads

Ontario

Ministry of Transportation and Communications

Research and Development Branch

87-01347/

Technical Report Documentation Page

Ultimate Soil Resistance of "Chance" Anchors and Concrete Footings for Horizontal Loads

Author:	F.W. Jung, Senior Research Engineer, Research & Development Branch, MTC
MTC No.:	HOS-86-01
Client Group:	Traffic Management & Engineering Office, Electrical Section Highway Design Office, Design & Development Section Engineering Materials Office, Foundation Design Office
Published by:	The Research and Development Branch Ontario Ministry of Transportation and Communications
Abstract:	Three-dimensional solutions for soil resistance from various authors were applied to cylindrical shaft foundations, and these were adjusted and extended to determine the ultimate load capacity against horizontal loads. Field tests were carried out under controlled soil conditions in cohesive and non-cohesive soils, using concrete cylinder shafts and cylindrical power-installed foundation anchors ("Chance" anchors) made of galvanized steel. At all increments of applied loads, the deflections were measured near ground level. At half the load capacity, the deflections were negligibly small in all test cases. The test results were compared with the mathematical modelling, and capacity equations were verified. The findings can be used to design footings for light poles, sign posts, and noise barrier columns.
Comments:	
Key words:	shallow caisson, foundations, three-dimensional solutions, cohesive soils, non-cohesive soils, footings, piles, shafts, power installed foundation anchors, noise barriers, noise barrier footings
Distribution:	Client group and foundation design engineers.
Copyright Status:	Crown copyright

HOS-86-01

Ultimate Soil Resistance of "Chance" Anchors and Concrete Footings for Horizontal Loads

F.W. Jung
Senior Research Engineer
Research and Development Branch, MTC

Published by
The Research and Development Branch
Ontario Ministry of Transportation and Communications
Hon. Ed Fulton, Minister
D.G. Hobbs, Deputy Minister

Published without prejudice as to the application of the findings. Crown copyright reserved; however, this document may be reproduced for non-commercial purposes with attribution to the Ministry.

For additional copies, write:
The Editor, Technical Publications
Room 320, Central Building
1201 Wilson Avenue
Downsview, Ontario
Canada M3M 1J8

Telephone: (416) 248-7226
CNCP Dialcom Electronic Mail: 21:MIN006

December 1986

TABLE OF CONTENTS

	PAGE
1/ INTRODUCTION	1
1.1/ The Challenge of Power-Installed Foundation Anchors	1
1.2/ Design Requirements	1
2/ LITERATURE ON THE SUBJECT	3
3/ EARTH PRESSURE EQUATIONS	4
4/ CAPACITY OF CYLINDRICAL SHAFTS IN COHESIONLESS SOILS, C_u=0, $\phi \neq 0$	10
5/ CAPACITY OF CYLINDRICAL SHAFTS IN COHESIVE SOILS, $C_u \neq 0$, ϕ=0	14
6/ FIELD TESTS, 1985/86	16
7/ INTERPRETATION OF FIELD TESTS, 1985/86	21
7.1/ Cohesive Soil, Clay (assume γ = 18 kN/m^3, C_u = 93 kPa)	21
7.2/ Cohesionless Soil, Silt (assume γ = 19.5 kN/m^3, ϕ = 41.5°)	21
7.3/ General Comparison	22
8/ CONCLUSIONS	23
REFERENCES	24
Acknowledgements	24
APPENDIX A/ Verification for Cohesionless and Cohesive Soils	25
APPENDIX B/ Solutions for "Chance" P.I.F.A.	27

LIST OF TABLES

PAGE

1/ Earth Pressure Coefficients K 9

2/ Functions a_ϕ, b_ϕ, and c 11

3/ Factors of Equation 15. 12

4/ Soil Test Results, Hamilton Test Site 17

5/ Soil Test Results, Ottawa Test Site 17

6/ Ottawa Test Results 18

7/ Hamilton Test Results 19

8/ Hamilton Tests Repeated, Summary of Test Results, May 1986. . . 20

9/ Influence of μ and ν. 22

LIST OF FIGURES

1/ Power Installed Foundation Anchor (Chance). 28

2/ Passive Earth Pressure Model. 29

3/ Increase in Earth Pressure from Cohesion at the Surface of the Caisson (Cylinder) 30

4/ Mechanism of Earth Resistance and Thrust in Cohesionless Soils (c = 0). 31

5/ Ultimate Stresses for Cohesionless Soils. 32

6/ Possible Ultimate Passive Soil Pressure for Cohesive Soils. . . 33

7/ Typical Installation of Test Mast 34

8/ Ottawa Tests in September 1985, Clay. 35

9/ Repeated Ottawa Tests in the Beginning of May, 1986, Clay . . . 36

10/ Hamilton Tests in September 1985, Silt 37

1/ INTRODUCTION

1.1/ The Challenge of Power-Installed Foundation Anchors (P.I.F.A.)

Traditional foundations for light poles, sign posts, and noise barrier columns consist of cylindrical concrete shafts. They were generously designed for "worst conditions" as it was considered less expensive to add a few cubic feet of concrete to the length of the shaft than to go to the trouble of investigating the actual soil conditions on the site.

Then came a new invention -- power-installed foundation anchors. The example shown in Figure 1 is the Chance Foundation Anchor, fabricated in Scarborough, Ontario. It consists of a cylindrical steel tube, a screw-shaped halo disc and pivoting steel bar at the bottom, and a flange disc at the top. The whole design is galvanized and can be augered into the ground directly, immediately prior to installing the light pole on top of it. There is no drilling, pouring, and curing of concrete weeks ahead of installation, as before. Thus, there are savings in installation costs, etc., whenever the soil conditions are favourable (as they usually are). Only soils featuring rocks, big boulders, or very hard clay are unsuitable.

To design installations using this anchor is more difficult than with traditional techniques because the engineer cannot be as generous with extra dimensions. The anchors are much smaller in diameter (6 to 10 in. compared to 26 in.) and depth cannot be generously added either. Therefore, it is necessary to design more closely to a failure load, and the theoretical basis for design equations must be three-dimensional to be sufficiently accurate.

1.2/ Design Requirements

There are two design requirements:

- by working stress limitations, avoid excessive deflections, and
- by an ultimate load capacity, a minimum of which must be provided to safeguard against overturning.

The required load capacity is about twice (1.85 times) the working stress load. In all tests it was demonstrated that the working stress load was accompanied by insignificantly small deflections and these, if they could be measured at all, were certainly elastic. Thus, it is suggested that design equations should be based on ultimate load capacity as derived in this report.

In tests where deflections were measured at ground level, it was found that, without exception, the deflections at half the ultimate load capacity were either zero or of the order of 5 mm or less, and were completely elastic. This means it is feasible to forego designing for working stress loads and deflection limitations.

Foundations of structures such as sign supports, light poles or columns of high mast lighting, and sound barriers must be designed for moments predominantly from horizontal wind loads. Such structural elements are also referred to as "footings" if they are small, and they have a cylindrical or prismatic shape. The material employed is usually ordinary concrete, but footings may also consist of pressure-treated timber or of coated/galvanized steel (as in the case of the Chance P.I.F.A.). The structural strength of those materials is assumed to be adequate. For a given dimension, such foundations have an ultimate load capacity depending on the properties of the soil.

For the aforementioned structures, the soil properties can be grouped into non-cohesive or cohesionless soils on the one hand, or cohesive soils on the other hand. The latter are assumed to be undrained and unconsolidated. Both assumptions (the total absence of cohesion or the presence of undrained and unconsolidated cohesive strength only) are conservative, resulting in minimum predicted load capacities. In the case of granular or non-cohesive soils, the water level below ground must be taken into account because the buoyancy of the water reduces the ultimate soil resistance considerably (however, this aspect is outside the scope of the present report).

This report presents physical/mathematical modelling for the ultimate load capacity prediction. It also presents results of physical tests performed under controlled conditions in typical Ontario soils. Actual failure loads measured are compared with model predictions in load deflection diagrams. The report deals only with uniform soil conditions and the results cannot be extended to several layers of soil with significantly different properties.

2/ LITERATURE ON THE SUBJECT

Numerous authors have proposed solutions designing laterally loaded shaft-type foundations. However, most of them do not offer a genuine three-dimensional solution, and sometimes they do not even include correction terms for the "wedge effect" in non-cohesive soils [2]. Other solutions are predominantly empirical (i.e., derived from test results) and they are useful for conditions within the test parameters. The solution offered in this paper, however, covers the whole range of soil classes for uniform soil conditions.

The solution for granular or cohesionless soils presented herein has been compared with various equations of other authors such as Meyerhof [5], and there was reasonable agreement based on less rigorous derivations. Typically, a capacity calculation according to Reference 5 is about 3% lower than according to the author's application of Berezantzev's solution.

The solution for cohesive soils has been checked against Reference 1. The most conservative assumption of the shape factor (with $k = 1.5$) matches fairly accurately with Coyle's proposed procedure. Coyle's method is supported by numerous test results and corresponds to an ultimate load based on 2% deflection or inclination of the shaft, which is not the highest possible load with angles of inclination beyond 2%. Refer to Appendix A for more details of verification.

3/ EARTH PRESSURE EQUATIONS

For cohesionless soils such as sand and gravel, the active or passive earth pressure (total earth resistance) is predominantly dependent on the angle of internal friction, ϕ. Cohesion may be present in loamy sands when moisture is present, but it is safe to neglect it. The angle ϕ changes with density and granular composition, but for any class of soil a conservative, low value can be assumed.

Cohesive soils such as clay are more complex in their behaviour of developing total earth resistance or passive earth pressures. For loads of short duration such as wind loads and for fully saturated soils, the cohesion, C_u , can be assumed to be independent of axial stresses, and the angle of internal friction can be neglected. In other words, all cohesive soils can be estimated in terms of a conservative value of cohesion, C_u, with $\phi = 0$.

In Reference 4, Equation 11.59, Page 301, a solution originally derived by Berezantzev (1953) is reported, which is based on a set of formulae for earth pressures on a vertical cylinder. The horizontal passive earth pressure, in reference to Figure 2, can be calculated as follows:

$$\sigma_{rp} = a\,\gamma\,\frac{\tan(45^\circ + \phi/2)}{\omega + 1}\left[\left(\frac{r_p}{a}\right)^{\omega+1} - 1\right] + q\left(\frac{r_p}{a}\right)^{\omega}\tan^2(45 + \phi/2) + c\cot\phi\left[\left(\frac{r_p}{a}\right)^{\omega}\tan^2(45 + \phi/2) - 1\right] \qquad (1)$$

where: $\omega = 2\tan\phi\tan(45 - \phi/2)$

$r_p = a + z\tan(45 + \phi/2)$

a = radius of the cylinder, in m

γ = specific weight of the soil, in kN/m^3

ϕ = angle of internal friction of the soil

q = surface load in kPa or kN/m^2

z = depth beneath the surface, in m.

Correspondingly, the active soil pressure is calculated by the following expression (Reference 4, Equation 11.58, page 300):

$$\sigma_{ra} = a\gamma \frac{\tan (45° - \phi/2)}{\lambda - 1} \left[1 - \left(\frac{a}{r_a}\right)^{\lambda-1}\right]$$

$$+ q \left(\frac{a}{r_a}\right)^{\lambda} + c \cot \phi \left[\left(\frac{a}{r_a}\right)^{\lambda} \tan^2 (45° - \phi/2) - 1\right] \qquad (2)$$

where: $\lambda = 2 \tan \phi \tan (45° + \phi/2)$

$r_a = a + z \tan (45° - \phi/2)$

An incremental movement of the cylindrical caisson from a horizontal load would activate passive soil pressure on one side and a very small amount of active soil pressure on the other side. The resulting force per unit length would be:

$$e = 2a (\sigma_{rp} - \sigma_{ra}) \qquad (3)$$

where: e = resulting force per unit length, in kN/m

σ_{rp} = passive soil pressure, in kPa

σ_{ra} = active soil pressure, in kPa

The resultant pressure, p, can be defined as:

$$p = \frac{e}{2a} = \sigma_{rp} - \sigma_{ra} \qquad (4)$$

For saturated cohesive soils, Equation 4 is only valid if there remains full contact on the side of active earth pressure, and there would be a resultant pressure $p = 4c$ for $\phi = 0$, and $q = 0$. This is invalid and only the passive earth pressure will be considered in this case. With $\phi = 0$ and $q = 0$ the last term of Equation 1 can be shown to become:

$$\sigma_r = \gamma z + 2c \qquad (5)$$

In Equations 1 to 5 there is the underlying assumption that the cohesion along the cylinder surface is zero. For cohesive soils this may be

regarded as overly conservative, especially when concrete is poured into an open drilled hole in the soil. In accordance with Reference 4, Equation 6.30a, (assuming $\beta = 90°$) the above Equation 5 is modified to:

$$\sigma_r = \gamma z + c (1 + \pi/2) = \gamma z + 2.57c \qquad (5a)$$

Equation 5 compared to Equation 5a implies a difference in the network of shear surfaces, leading to an increase in earth resistance as illustrated in Figure 3. The shear surfaces pertaining to Equation 5a start horizontally instead of under an angle of $45° + \phi/2$, and correspondingly at the rough surface of the cylinder there is $c = c_u$ instead of $c = 0$.

The last term of Equation 5, according to Meyerhof et al, is increased by a shape factor, S_c (Reference 5). From Figure 10 in Reference 5, it can be seen that test results should be taken into account in estimating this factor. A conservative estimate of the shape factor, S_c, would be (with $B = 2a$):

$$S_c = 1 + k \log (1 - z/B) \quad \leq 3 \qquad (6)$$

For design purposes, Equations 5 and 6 are combined to

$$\sigma_r = \gamma z + 2 c S_c \qquad (7)$$

In Equation 6 the term k is a coefficient matching the experimental results by Meyerhof et al [5]. Assume:

k = 2 for the theoretical curve shown in [5]
k = 1.7 for a curve through experimental results (mean)
k = 1.5 for a more conservative curve, matching Reference 1

It should be noted that the solutions are also valid for other than circular shapes. In this case $2a = B$ (where B = the width lateral to the direction of P, in m).

Equation 7 will be used to determine the depth of footings in cohesive soils. These soils are assumed to be saturated, as a worst condition,

and the internal angle of friction is then assumed to be zero. At the same time it is safe to neglect the active part of the earth pressure.

For cohesionless soils the cohesion (c) is assumed to be zero, and Equation 4 in conjunction with Equations 1 and 2 will be used to calculate footings in this kind of soil, q and c being zero. Thus, for cohesionless soils:

$$p = a\,\gamma\,(F_p - F_a) \tag{8}$$

where: $F_p = \tan(45° + \phi/2)\left[\left(\frac{r_p}{a}\right)^{\omega+1} - 1\right]/(\omega + 1)$

$$F_a = \tan(45° - \phi/2)\left[1 - \left(\frac{a}{r_a}\right)^{\lambda-1}\right]/(\lambda - 1)$$

$$\omega = 2 \tan\phi \tan(45° - \phi/2)$$
$$\lambda = 2 \tan\phi \tan(45° + \phi/2)$$
$$r_p = a + z \tan(45° + \phi/2)$$
$$r_a = a + z \tan(45° - \phi/2)$$

The term F_a in Equation 8 is very small compared to F_p, but it may be significant enough, especially for smaller angles of internal friction (ϕ) and small ratios of z/a. To neglect the term F_a would be unconservative. Instead, it is suggested that K, a combined earth pressure coefficient, be derived. K is defined as follows:

$$K = \frac{p}{z\gamma} = (F_p - F_a)\,\frac{a}{z} \tag{9}$$

Since Equation 8 is valid for cylindrical and other prismatic foundations, the variable z/a is replaced by (z/B) = 0.5 (z/a), where B = 2a, which is the dimension of the footing perpendicular to the load. Table 1 has been calculated based on Equations 8 and 9.

Using the earth pressure coefficient from Equation 9, the pressure (p) is:

$$p = \gamma\, z\, K \tag{10}$$

The mechanical effect of earth pressure loads on shallow caissons is illustrated in Figure 4. The caisson is suffering an incremental twist around T under the horizontal loads M (moment) and Q (shear force). This activates the earth pressures as shown, in accordance with Equations 8 and 9. The combined pressure (p) is acting in opposite directions above and below T, balancing the forces M and Q.

Earth pressure coefficients based on Equation 9 have been calculated for a range of ratios, Z/B and internal friction angles, ϕ. The results are listed in Table 1, which can be used as a basis for an evaluation of overturning moment capacities of cylindrical shaft formations in non-cohesive soils.

Refer also to Appendix A for comparison with previously-derived methods.

Table 1/ Earth Pressure Coefficients K

z/B	ϕ=25°	27.5°	30°	32.5°	35°	37.5°	40°
0	2.033	2.334	2.655	3.012	3.410	3.858	4.365
0.2	2.548	2.938	3.378	3.879	4.454	5.122	5.904
0.4	2.972	3.455	4.006	4.643	5.385	6.258	7.295
0.6	3.354	3.922	4.579	5.345	6.246	7.316	8.600
0.8	3.704	4.354	5.112	6.002	7.057	8.320	9.844
1	4.030	4.759	5.615	6.625	7.830	9.280	11.039
1.2	4.336	5.143	6.093	7.221	8.573	10.205	12.196
1.4	4.628	5.508	6.550	7.794	9.289	11.102	13.320
1.6	4.905	5.858	6.991	8.347	9.983	11.974	14.416
1.8	5.172	6.196	7.417	8.883	10.658	12.824	15.488
2	5.429	6.522	7.829	9.405	11.317	13.656	16.538
2.2	5.677	6.822	8.231	9.913	11.961	14.470	17.570
2.4	5.917	7.145	8.622	10.410	12.591	15.270	18.584
2.6	6.150	7.444	9.003	10.897	13.209	16.055	19.582
2.8	6.377	7.735	9.377	11.373	13.817	16.828	20.566
3	6.598	8.020	9.742	11.841	14.413	17.589	21.537
3.2	6.814	8.299	10.101	12.300	15.001	18.339	22.495
3.4	7.025	8.572	10.453	12.752	15.580	19.079	23.442
3.6	7.232	8.840	10.799	13.197	16.150	19.810	24.377
3.8	7.434	9.103	11.139	13.635	16.713	20.532	25.303
4	7.633	9.362	11.474	14.067	17.269	21.246	26.219
4.2	7.828	9.616	11.804	14.493	17.818	21.952	27.127
4.4	8.019	9.866	12.129	14.914	18.360	22.650	28.025
4.6	8.208	10.113	12.449	15.329	18.897	23.342	28.916
4.8	8.393	10.356	12.766	15.740	19.428	24.027	29.799
5	8.575	10.595	13.078	16.146	19.953	24.705	30.675

ϕ = internal angle of friction.

4/ CAPACITY OF CYLINDRICAL SHAFTS IN COHESIONLESS SOILS, C_u=0, $\phi \neq 0$

To determine the overturning capacity of cylindrical shaft foundations, it is necessary to integrate blocks of soil pressure along the depth of the shaft, as shown in Figure 5. At the same time, it is necessary to estimate or assume the depth, νD, of the activated upper soil pressure area, and the depth, μD, of the resultant soil resistance force at the bottom. The earth resistance is a force per unit length along the shaft, namely B•p, where p is given by Equations 9 and 10.

In order to carry out the integration, the following approximation is made.

A/ Each column in Table 1 represents a function of the earth pressure coefficient K and is approximated by the following expression:

$$K_\phi = a_\phi + b_\phi \zeta^c \tag{11}$$

where: $\zeta = \frac{z}{B}$ (12)

a_ϕ, b_ϕ, c = functions of ϕ

Taking the bending moments around the point B near the bottom, the following equation can be established in reference to Figure 5:

$$P_u(H + \mu D) = \int_0^{\nu D} (Bp)(\mu D - z)dz \tag{13}$$

where: $(Bp) = B\gamma z K_\phi$ (14)

The solution of this set of equations, 11 to 14, leads to the following expression for P_u:

$$P_u = \frac{\gamma B D^3}{H + \mu D} \cdot \left[a_\phi\left(\frac{\mu\nu^2}{2} - \frac{\nu^3}{3}\right) + b_\phi\left(\frac{\mu\nu^{c+2}}{c+2} - \frac{\nu^{c+3}}{c+3}\right)\left(\frac{D}{B}\right)^c\right. \tag{15}$$

where: P_u = ultimate overturning force, in kN

H = lever arm of force P_u above ground level, in metres

D = depth of shaft, in metres

B = diameter of shaft, in metres

γ = specific weight of soil, in kN/m^3

μ = parameter, so that μD is the depth or level of the resultant soil resistance at the bottom of the shaft

ν = parameter, so that νD is the depth, z, of the activated soil stress at the upper part of the shaft

The parameters μ and ν must be assumed, and the functions a_ϕ, b_ϕ, and c can be taken from the following Table 2, which is based on curve fitting through the points ζ = 0, 2.4, and 5 with respect to Table 1.

Table 2/ Functions a_ϕ, b_ϕ, and c

	a_ϕ	b_ϕ	c
25°	2.033	2.0853	0.7104
27.5°	2.334	2.5244	0.7366
30°	2.655	3.0681	0.7598
32.5°	3.012	3.7302	0.7821
35°	3.410	4.5487	0.8022
37.5°	3.858	5.5622	0.8209
40°	4.365	6.8250	0.8384

B/ Between ϕ = 28° and ϕ = 35° the functions a_ϕ, b_ϕ, and c can approximated by the following expressions:

$$a_\phi = \frac{\phi}{7} - 1.63 \qquad (16)$$

$$b_\phi = 0.2 + \phi^3/9300 \qquad (17)$$

$$c = 0.75 = \text{constant} \qquad (18)$$

for angles of ϕ between 28° and 35°, Equations 16, 17, and 18 can be used instead of actual or interpolated values from Table 2. This leads to sufficiently accurate results for P_u, when used in Equation 15. For C = 0.75 being constant, Table 3 can be used to select factors with regard to the parameter μ and ν.

Table 3/ Factors of Equation 15

Level of Assumption	μ	ν	$(\frac{\mu\nu^2}{3} - \frac{\nu^3}{3})$	$(\frac{\mu\nu^{c+2}}{c+2} - \frac{\nu^{c+3}}{c+3})$
progressive	0.94	0.80	0.1301	0.0696
medium	0.92	0.775	0.1211	0.0634
conservative	0.90	0.75	0.1125	0.0570

C/ Between ϕ = 24° and ϕ = 45° the functions a_ϕ, b_ϕ, and c_ϕ can be closely approximated by the following equations:

$$a_\phi = 2.033 + 0.1056(\phi - 25) + 0.0033244(\phi - 25)^2 \quad (19)$$

$$b_\phi = 2.0853 + 0.12266(\phi - 25) + 0.012888(\phi - 25)^2 \quad (20)$$

$$c_\phi = 0.7104 + \frac{\phi - 25}{94.4644} - \frac{(\phi - 25)^2}{7305.67} \quad (21)$$

Equations 19, 20 and 21 are more accurate than Equations 16, 17 and 18; therefore they are more suitable for PC or micro-computer programming.

Example

$H = 2.5$ m, $D = 2.0$ m, $B = 0.5$ m

$\mu = 0.90$, $\nu = 0.75$, $\phi = 35°$

$\gamma = 20$ kN/m^3 dense soil, conservative assumption for μ and ν.

$$P_u = \frac{20 \times 0.5 \times 2.0^3}{2.5 + 0.9 \times 2.0} [3.410 \times 0.1125(\text{Table 3}) + 4.5487]$$

$$\times \left(\frac{0.9 \times 0.75^{2 \cdot 8022}}{2.8022} - \frac{0.75^{3 \cdot 8022}}{3.8022}\right) \left(\frac{2.0}{0.5}\right)^{0 \cdot 8022}]$$

$$P_u = \frac{80}{4.3} [0.3836 + 0.2517 \times 4^{0 \cdot 8022}]$$

$$= 18.605 [1.1489]$$

$$= \underline{21.4 \text{ kN}}$$

Or, using Equations 16, 17, and 18:

$$P_u = 18.605 [3.37 \times 0.1125 + 4.81 \times 0.057 \times 4^{0 \cdot 75}]$$

$$= 18.605 [1.1546]$$

$$= \underline{21.5 \text{ kN}}$$

Or, using Equations 19, 20, and 21:

$$P_u = 18.605 [3.42144 \times 0.1125 + 4.6007 \times 0.055324 \times 4^{0 \cdot 802572}]$$

$$= 18.605 [1.15926]$$

$$= \underline{21.6 \text{ kN}}$$

5/ CAPACITY OF CYLINDRICAL SHAFTS IN COHESIVE SOILS, $C_u \neq 0$, $\phi = 0$

Based on the soil pressure as given in Equations 6 and 7, a simpler stress block model can be used to determine the turnover capacity in cohesive soils. This model is illustrated in Figure 6. Taking the bending moments around points A and B respectively, the following two sets of equations can be derived, where C is the undrained and unconsolidated shear strength of the soil, in kPa:

$$P_{u_2} = \frac{0.30BD^2\sigma_1}{H + 0.85D} \tag{22}$$

where: $\sigma_1 = 0.3\gamma D + 2C_u S_1$ (23)

where: $S_1 = 1 + k \log(1 + 0.3\ D/B) \quad < 3$ (24)

$$P_{u_2} = \frac{0.15BD^2\sigma_2}{H + 0.35D} \tag{25}$$

where: $\sigma_2 = 0.85\gamma D + 2C_u S_2$ (26)

where: $S_2 = 1 + k \log(1 + 0.85\ D/B) \quad < 3$ (27)

The capacity, P_u, in kN, is the lesser of the two values calculated by Equations 22 and 25.

Refer to Appendix A for comparison with Reference 1.

Example

H = 2.5 m, D = 2.0 m, B = 0.5 m
k = 1.5, conservative in order to limit deflection
γ = 20 kN/m^3

a) C_u = 25 kPa, soft to firm clay
P_u = 12.40 kN = P_{u_2}
(P_{u_1} = 12.53 > 12.40, not controlling)

b) C_u = 50 kPa, firm to stiff clay
P_u = 21.61 kN = P_{u_2}
(P_{u_2} = 23.34 > 21.61, not controlling)

c) C_u = 12 kPa soft clay
P_u = 6.90 kN = P_{u_1}
(P_{u_2} = 7.61 kN > 6.90, not controlling)

P_{u_1} seems to be the smaller value only if values of C_u are very low (< 25 kPa).

6/ FIELD TESTS, 1985/86

Two test sites were selected for controlled tests on cylindrical concrete shaft foundations and power-installed Chance foundation anchors. One site, in Hamilton, Ontario, featured a non-cohesive soil, i.e., silt with a relatively high angle of internal friction. Results of the soil investigation are listed in Table 4. Another test site was chosen near Ottawa, representing a cohesive soil, i.e., clay. The soil test results are listed in Table 5.

A typical installation of the tests is shown in Figure 7. The foundations were tested in pairs by pulling the top of two 3 m high steel masts towards one another, generating increments of the horizontal force (P) by a hydraulic jack. A summary of the test results is presented in Tables 6, 7, and 8.

To evaluate the test results, it is important to look at load deflection diagrams, using "settled down" deflections after each increment of load. Such diagrams are presented in Figures 9, 10, and 11. The deflections were measured at ground level (flange plates).

More detailed descriptions and results of the field tests are presented in Appendix B.

Table 4/ Soil Test Results, Hamilton Test Site

				ATTERBERG LIMITS								
FIELD NO.	DEPTH INCHES	TYPE	W %	WL %	WP %	IP %	P.C.F.	INTERNAL ANGLE OF FRICTION	GRAIN SIZE			
									GR	SA	Si	CL
1	0-12	SS	22.5									
2	12-24	SS							0.0	4.5	85.5	10.0
3	24-36	SS										
4	26-48	SS										
5	48-60	SS	25.0				123.0	41.5	0.0	7.5	85.5	7.0
6	60-72	SS										
7	72-84	SS										
8	84-96	SS	22.0						0.0	4.5	89.5	6.0
9	96-108	SS										

Table 5/ Soil Test Results, Ottawa Test Site

				ATTERBERG LIMITS								
FIELD NO.	DEPTH INCHES	TYPE	W %	WL %	WP %	IP %	P.C.F.	SHEAR STRENGTH Psf	GRAIN SIZE			
									GR	SA	Si	CL
1	0-28	TW	33.5	70.5	23.5	47.0	109.0	1015.0	0.0	3.5	46.5	51.0
2	28-45	TW	33.0	66.5	23.5	43.0	117.0	3205.0	0.0	1.0	38.5	60.5
3	45-73	TW	42.5	69.5	20.5	49.0	115.0	975.0	0.0	0.0	31.0	69.0
4	73-93	TW	40.5	69.0	22.5	45.5	113.0	1985.0				
5	93-113	TW	44.0	70.0	18.5	51.5	112.0	1850.0	0.0	6.0	49.5	44.5
6	113-135	TW	36.0	70.0	26.0	44.0	116.0	1790.0	0.0	15.5	66.0	18.5

W - % Moisture
WL - Liquid limit
WP - Plastic limit
IP - Index of plasticity
P.C.F. - Pounds per cubic foot
GR - Gravel
SA - Sand
Si - Silt
CL - Clay
SS - Sandy Silt
TW - Wet Clay

Table 6/ Ottawa Test Results

TEST NO.	TYPE OF FOUNDATION	ULTIMATE FAILURE LOAD P_u	DEFLECTION AT GROUND LEVEL (P_u)	PREDICTED ULTIMATE LOAD CAPACITY	H (m)	D (m)	B (m)
** 1	CHANCE 6 in. x 6 ft. .152 x 1.829	4000 lb 17.8 kN	17.14 mm	2686 lb 11.65 kN	3.10	1.70	0.170
** 2	CHANCE 8 in. x 6 ft. .203 x 1.829	5000 lb 22.2 kN	16.27 mm	3310 lb 14.12 kN	3.15	1.65	0.221
3	CONCRETE 26 in. x 5 ft. .660 x 1.524	7000 lb 31.1 kN	14.05 mm	5437 lb 24.185 kN	3.00	1.50	0.66
4	CONCRETE 26 in. x 8 ft. .660 x 2.438	anchorage assembly failure at 11000 lb	--	15000 lb 66.87 kN	3.00	2.40	0.66

**S = 3 (assumed)

ζ = 18 kN/m^3

C_u = 93 kPa (near bottom)

Table 7/ Hamilton Test Results

TEST NO.	TYPE OF FOUNDATION	ULTIMATE FAILURE LOAD P_u	DEFLECTION AT GROUND LEVEL (P_u)	PREDICTED * ULTIMATE LOAD CAPACITY	H m	D m	B m
5	CHANCE 6 in. x 6 ft. .152 x 1.829	4000 lb 17.8 kN	23.95 mm	3874 kN 17.23 kN	3.15	1.65	0.170
6	CHANCE 8 in. x 6 ft. .203 x 1.829	5000 lb 22.2 kN	13.72 mm	4660 lb 20.73 kN	3.10	1.7	0.221
7	CONCRETE 26 in. x 5 ft. .660 x 1.524	6000 lb 26.7 kN	11.715 mm	4772 lb 21.23 kN	2.95	1.50	0.66
8	CONCRETE 26 in. x 8 ft. .660 x 2.438	anchorage assembly failure at 9000 lb	--	20.968 kN 93.27 kN	3.05	2.40	0.66

*$\mu = 1$, $\nu = 1$

$\gamma = 19.5$ kN/m^3

$\phi = 41.5°$

H = height of P_u above ground, m

D = effective depth of footing, m

B = shaft diameter, m

Table 8/ Ottawa Tests Repeated, Summary of Test Results, May 1986

TEST NO.	TYPE OF FOUNDATION	ULTIMATE FAILURE LOAD P_u	DEFLECTION AT GROUND LEVEL (P_u)	PREDICTED * ULTIMATE LOAD CAPACITY	H m	D m	B m
9	CHANCE 6 in. x 6 ft. .152 x 1.829	3500 lb 15.57 kN	21.2 mm	2736 kN 12.16 kN*	3.05	1.727	0.170
10	CHANCE 8 in. x 6 ft. .203 x 1.829	4500 lb 20.02 kN	21.3 mm	3372 lb 15.00 kN*	3.09	1.689	0.221
11	CONCRETE CYLINDER 26 in. x 6 ft. .660 x 1.829	3500 lb 5.57 kN	11.0 mm	8500 lb 37.78 kN	2.95	1.829	0.660

*S = 3 (assumed)

γ = 18 kN/m^3

C_u = 93 kPa (near bottom)

Note: Test 11 shows inexplicable premature failure.

7/ INTERPRETATION OF FIELD TESTS 1985/86

7.1/ Cohesive Soil, Clay (assume γ = 18 kN/m^3, C_u = 93 kPa)

The predicted ultimate load capacity for each test in the clay soil near Ottawa is listed in Tables 6 and 8. The calculations were carried out in accordance with Equations 22 to 27. All the cases of Chance foundation anchors were calculated with a value of S_2 = 3 because of their slenderness.

The load versus stabilized deflection diagrams are shown in Figures 8 and 9 for the September and May tests, respectively. The predicted failure loads are indicated by black triangles. Note that these loads are close to a region of increased rate of deflection but well below the ultimate failure loads at the end of the diagrams. The same soil parameters (ζ = 18 kN/m^3, C_u = 93 kPa) were used for the original test in fall 1985 and the repeated tests in spring 1986. In spite of the softening of the top layer in the spring, the formulae for prediction (Equations 19 to 24) still hold, although with a reduced margin to ultimate failure. Note that the ultimate failure is defined by the fact that deflections "creep on", i.e., they do not settle down to a final value after the last increment of load, after one hour.

7.2/ Cohesionless Soil, Silt (assume γ = 19.5 kN/m^3, ϕ = 41.5°)

The predicted ultimate load capacity for each test in the silty soil near Hamilton is listed in Table 7. The calculations were carried out in accordance with Equations 15, 19, 20, and 21, with a non-conservative assumption of μ = 1 and ν = 1 (Figure 6).

Figure 10 contains the predicted failure load indicated by black, solid pyramids. With this assumption of μ and ν equal to unity there is still some margin for ultimate failure. It should be interesting to study a more conservative assumption for μ and ν, such as in accordance with the values in Table 3. The results are listed in Table 9.

Table 9/ Influence of μ and ν

TEST	FAILURE LOAD	$\mu = 1$ $\nu = 1$	$\mu = 0.94$ $\nu = 0.80$	$\mu = 0.92$ $\nu = 0.775$	$\mu = 0.90$ $\nu = 0.75$
5. Chance F.A. 6" x 6'	17.8 (4000)	17.23 (3873)	12.65 (2844)	11.63 (2615)	10.66 (2396)
6. Chance F.A. 8" x 6'	22.2 (5000)	20.73 (4660)	15.27 (3433)	14.05 (3159)	12.89 (2898)
7. Concrete Shaft 26" x 5'	26.7 (6000)	21.23 (4773)	15.92 (3579)	14.71 (3307)	13.56 (3048)

*dimensions: kN, (lb.)

For the most conservative assumption, $\mu = 0.90$ and $\nu = 0.75$, the predicted failure points are indicated by non-solid pyramids in the diagrams of Figure 10. The loads are roughly half of the ultimate failure loads. However, there is a disproportionately large reduction in deflection (down to about one-third).

7.3/ General Comparison

Prediction calculations compared with test results as plotted in Figures 8, 9 and 10 clearly reveal the limitations of predictions and the meaning of the equations presented. In general, it has been proven that the presented soil-shaft interaction model underlying the prediction equations is correct: with increasing deflection, more and more soil is being engaged in providing resistance against overturning of the footings. In particular, there is a tremendous capacity in granular, non-cohesive soils against overturning: up to $\mu = 1$ and $\nu = 1$ and apparently even higher because of some small neglected cohesion. Cohesive soils weaken in the spring, but not sufficiently to render the prediction equations invalid.

8/ CONCLUSIONS

Equations have been derived to estimate the capacity of shallow caisson foundations for overturning (horizontal) forces. The equations are derived from basic principles of soil mechanics, and approximations have been introduced, to achieve sets of simple design equations that can be used by the foundation engineer in solving practical problems. The author has endeavoured to illustrate clearly the underlying mechanics of soil behaviour and maintain the visibility of assumptions. The selection of parameters (such as ϕ, C_u, γ, μ, and ν) is left to the judgement of the expert engineer, in accordance with prevailing conditions. For instance, Chance anchors with their wide "halo" disc and pilot blade at the bottom may be designed with larger values of μ and γ than cylindrical concrete foundations.

On the other hand, uncertainties in determining soil parameters (ϕ and C_u) and variations in soil conditions may require that such parameters be factored down, in accordance with common practice. Overturning moments or loads must be applied with a load factor corresponding to an ultimate limit slate design in structural analysis. However, such material and load factors should be selected carefully, also in accordance with the level of risk in case of failure. These and similar decisions must be left to the practising engineer.

To verify the ultimate load prediction model, eleven tests were carried out under controlled soil conditions. Two of these tests, on concrete shafts, failed prematurely at the connection of the steel column to the concrete. The concrete reinforcement failed. All other tests showed failure loads above the predicted ones.

REFERENCES

[1] Coyle, H. M., et al, "Design of Rigid Shafts in Clay for Lateral Loads," Journal of Geotechnical Engineering, V. 109, No. 9, September 1983.

[2] Ivey, Don L., "Signboard Footings to Resist Wind Loads," Civil Engineering, ASCE, December 1966.

[3] Jung, F. W., "Shallow Caisson Foundations for Light Poles, Sign Posts and Noise Barrier Columns", Ministry of Transportation and Communications, Ontario, R&D Report M-82-01, December 1981.

[4] Kezdi, Arpad, "Erddruck-Theorien" -- "Theories of Earth Pressure," Springer, Verlag, Berlin, 1962.

[5] Meyerhof, G. G., et al, "Lateral Resistance and Deflection of Rigid Walls and Piles in Layers Soils," Canadian Geotechnical Journal, V. 18, 1981.

[6] Brohms, Bengt B., "Lateral Resistance of Piles in Cohesive Soils," Proc. A.S.C.E., Soil Mechanics and Foundation Division, March 1964.

[7] Brohms, Bengt B., "Design of Laterally Loaded Piles," Proc. A.S.C.E., Soil Mechanics and Foundation Division, May 1965.

ACKNOWLEDGEMENTS

Appreciation is extended to Mr. A. Titishov and to Mr. L. Crowder for their contributions in carrying out all the field tests of fall, 1985, and spring, 1986, and for processing the test data.

APPENDIX A/ Verification for Cohesionless and Cohesive Soils

Verification for Cohesionless (Granular) Soils

The solution for the ultimate soil resistance has been checked against a formula given in "Taschenbuch fuer Bauingenieure", Schleicher, Second Edition, Volume 2, p. 136. This old formula takes into account the widening wedge of the granular soil with depth at ultimate load, in a conservative approximate way. Comparisons for the following parameters are presented:

B = 2 ft, $\phi = 30°$, $\gamma = 120$ psf

Depth z	$p = \gamma z K$	Schleicher [6]	Note:
2.38 ft	1714 psf	1537 psf	determine K
3.06 ft	2534 psf	2225 psf	from Table 1
4.76 ft	4855 psf	4433 psf	
7.20 ft	9850 psf	8813 psf	

The difference is about 10 to 15%, which is a reasonable verification of the Berezantzev solution.

Verification for Cohesive Soils

Reference 1, a more recent publication of the "Design of Rigid Shafts in Clay for Lateral Loads" offers a procedure for a limit stress design by 2% deflection or shaft inclination. Fairly accurate correspondence can be established by setting k = 1.5 in Equation 6. Results of comparative calculations are presented for the following three examples:

1/ B = 0.457 m, D = 2.5 m, H = 2 m, C_u = 150 kN/m
Capacity P_u = 101.155 kN (author's)
P_u = 101.13 kN (Reference 1)

2/ B = 0.457 m, D = 1.5 m, H = 2 m, C_u = 100 kN/m
Capacity P_u = 12.890 kN (author's)
P_u = 13.7 kN (Reference 1).

3/ B = 0.610 m, D = 3 m, H = 2 m, C_u = 100 kN/m
Capacity P_u = 121.333 kN (author's)
P_u = 118.9 kN (Reference 1).

There is a perfect correspondence in view of the fact that the calculations based on Reference 1 depend on reading values from a very small diagram.

APPENDIX B/ Solutions for "Chance" P.I.F.A.

Ultimate Capacity in Non-Cohesive Soils

With reference to Figure 1, the following equations have been derived to calculate the ultimate load capacity, P_u, from balancing bending moments. For non-cohesive soils, the moments are being balanced around a point at the bottom, at the level of the force, Q, which is assumed to act at the centre of the screw disc. Assume $\nu = 1$ and $\mu = 1$.

$$A = \frac{\phi}{7} - 1.63$$

$$E = 0.20 + \frac{\phi^3}{9300}$$

$$K = 0.167A + 0.097E \left(\frac{D}{B}\right)^{0.75}$$

$$P_u = \frac{\zeta B D^3 K}{H + D}$$

where: P_u = ultimate load, in kN
H = lever arm of P_u above ground, in metres
D = length of shaft, in metres
B = outside shaft diameter, in metres
ζ = specific weight of soil, in kN/m
ϕ = angle of internal friction of soil

Ultimate Capacity in Cohesive Soils

The following equations can be used to estimate the ultimate load capacity in cohesive soils:

$$F = 0.85\zeta D + 2C_u S$$

$$P_u = \frac{0.15\ B D^2 F}{H + 0.35D}$$

where: C_u = undrained and unconsolidated shear strength, in kPa
S = shape factor according to Meyerhof.

The shape factor, S, can be expected to be between three and four, for the relatively slender Chance foundation anchors. Thus, assume S = 3.0.

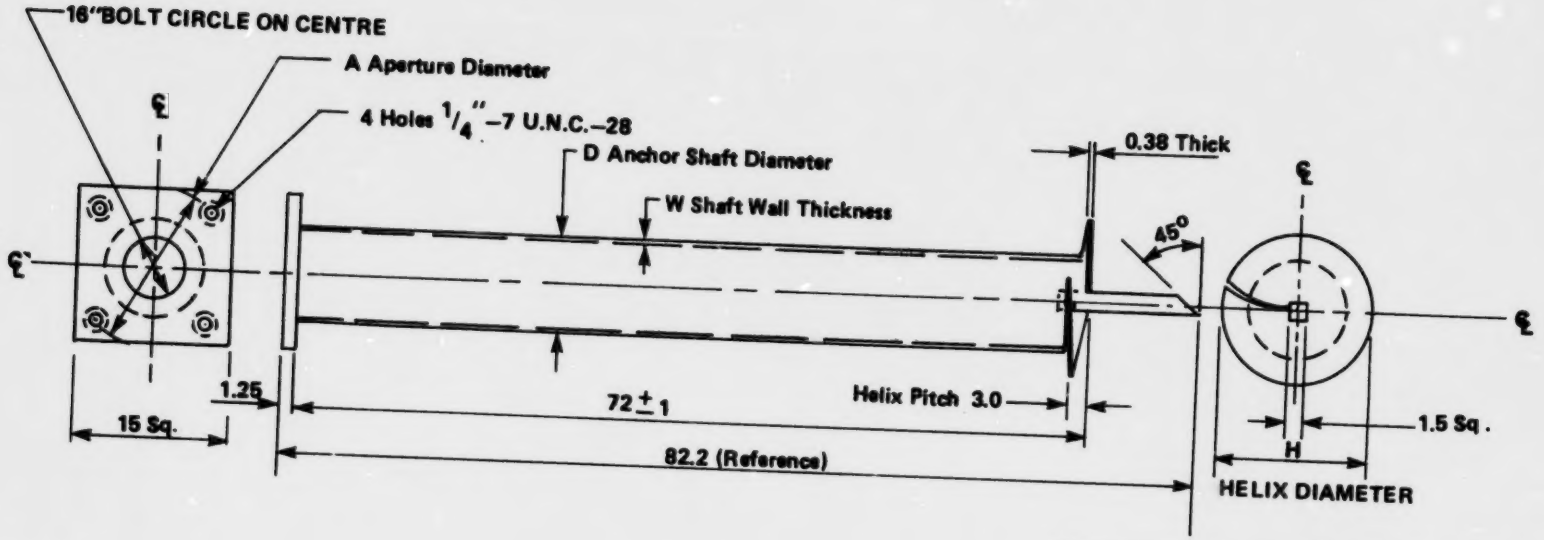

Figure 1/ Power Installed Foundation Anchor (Chance)

TABLE SHOWING VARIABLE DIMENSIONS FOR TEST ANCHORS
ALL OTHER DIMENSIONS ARE TYPICAL

TEST ANCHOR DESCRIPTION	DIMENSIONS (Inches)			
	A	D	H	W
No. 1, 8 in. x 6 ft.	7.0	8.63	13.5	0.25
No. 2, 8 in. x 6 ft.	5.0	6.51	11.5	0.25

NOTE: All dimensions are in inches (1 inch = 2.54 cm)

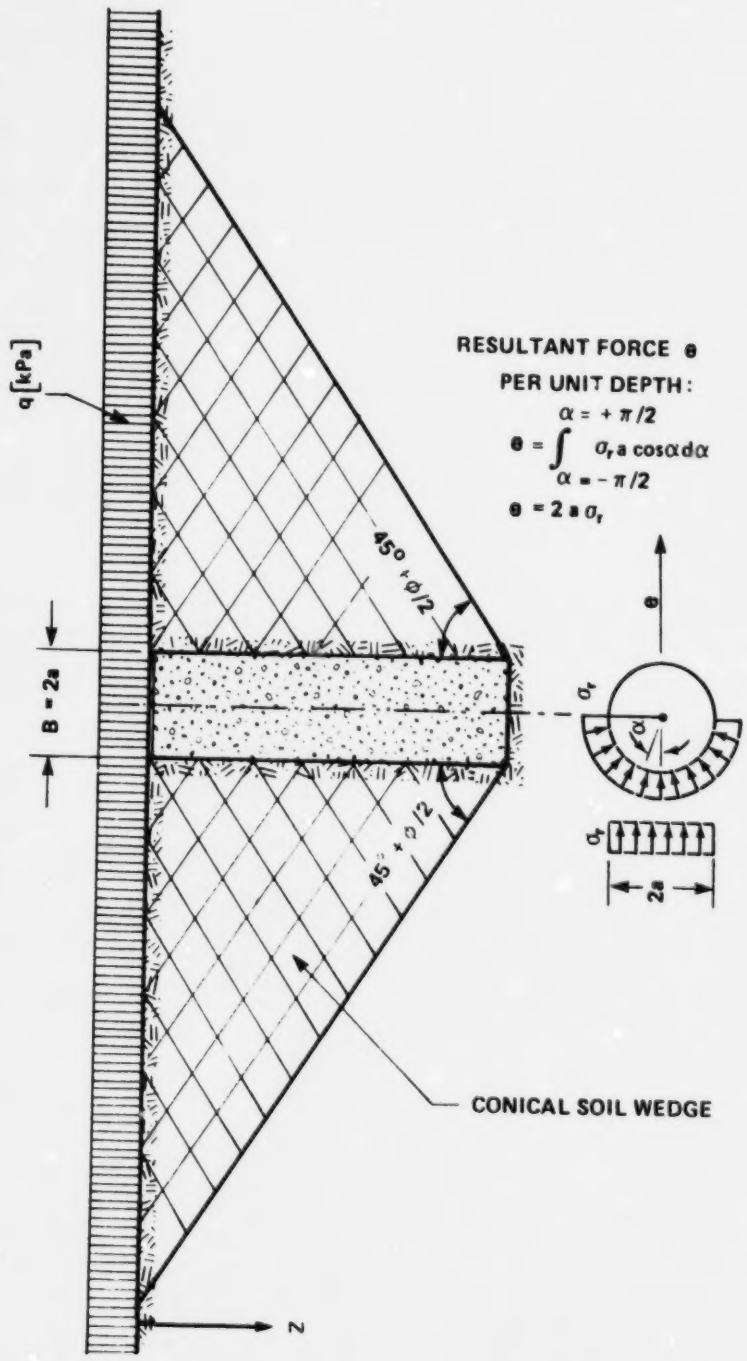

Figure 2 / Passive Earth Pressure Model

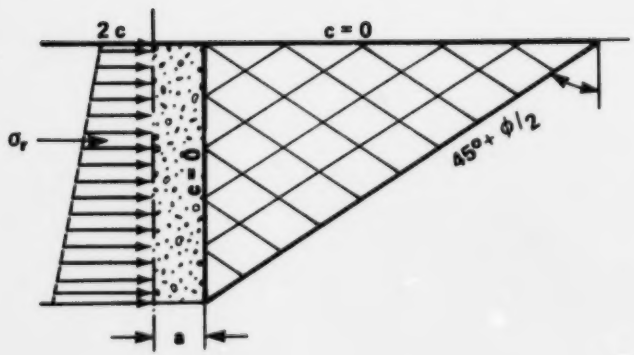

for $\phi = 0$: $\sigma_r = \gamma z + 2\,c\,s_c$ (5)

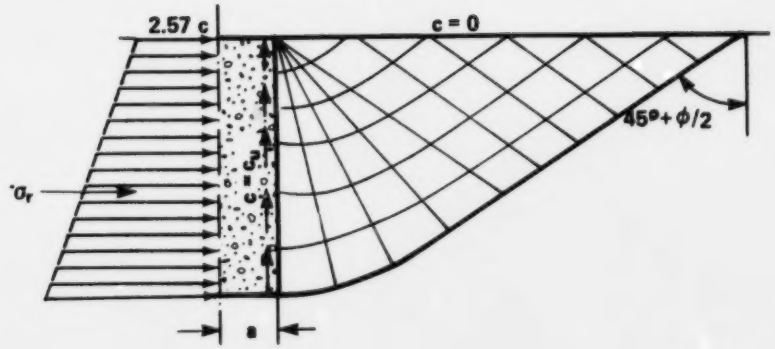

$\sigma_r = \gamma z + 2.57\,c\,s_c$ (6)

Figure 3/ Increase in Earth Pressure from Cohesion at the Surface of the Caisson (Cylinder)

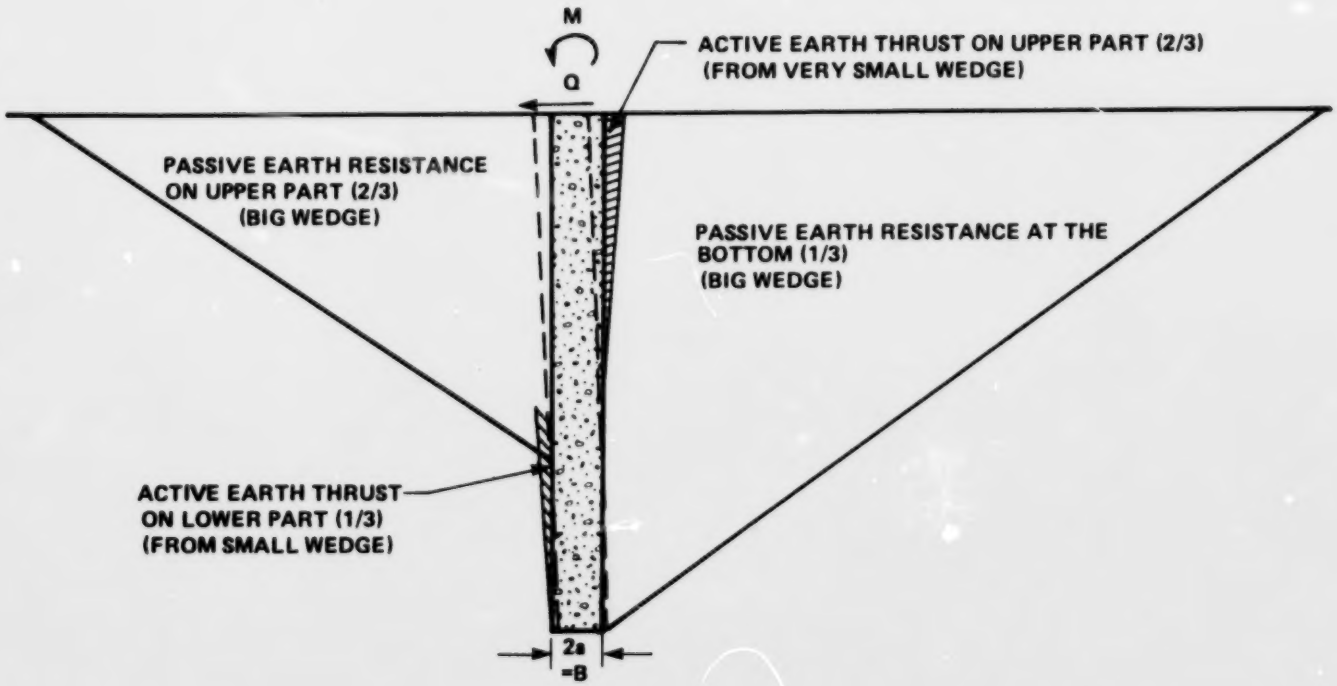

Figure 4/ Mechanism of Earth Resistance and Thrust in Cohesionless Soils (C=0)

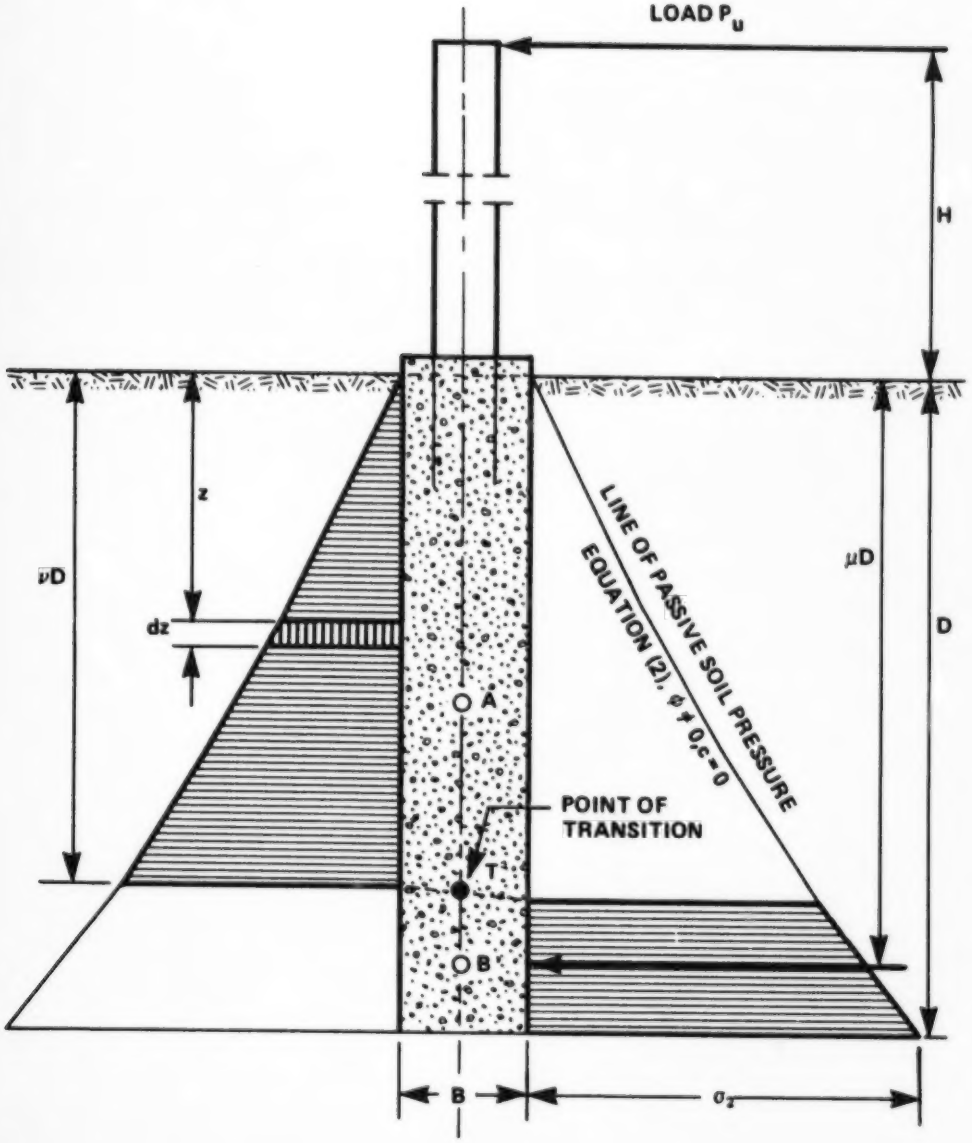

Figure 5/ Ultimate Stresses for Cohesionless Soils

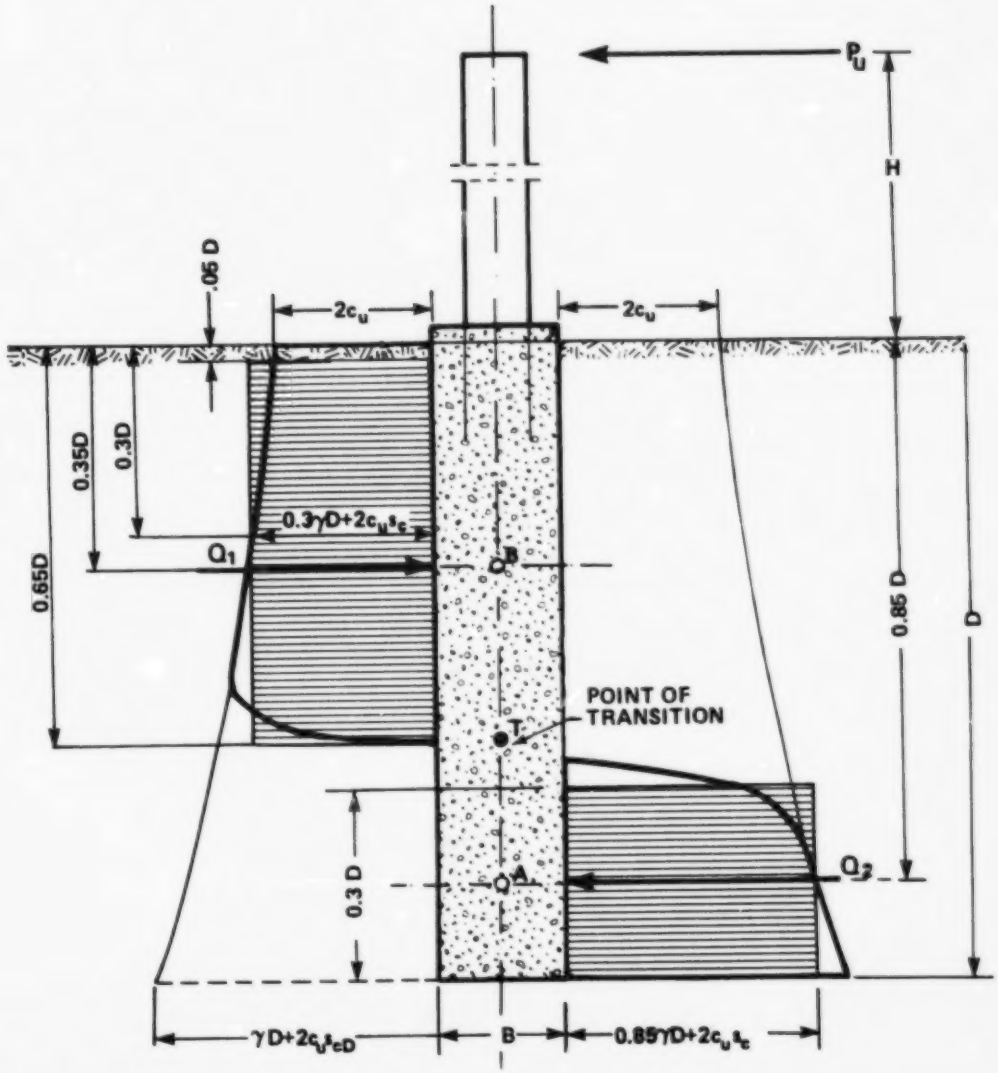

Figure 8/ Possible Ultimate Passive Soil Pressure for Cohesive Soils

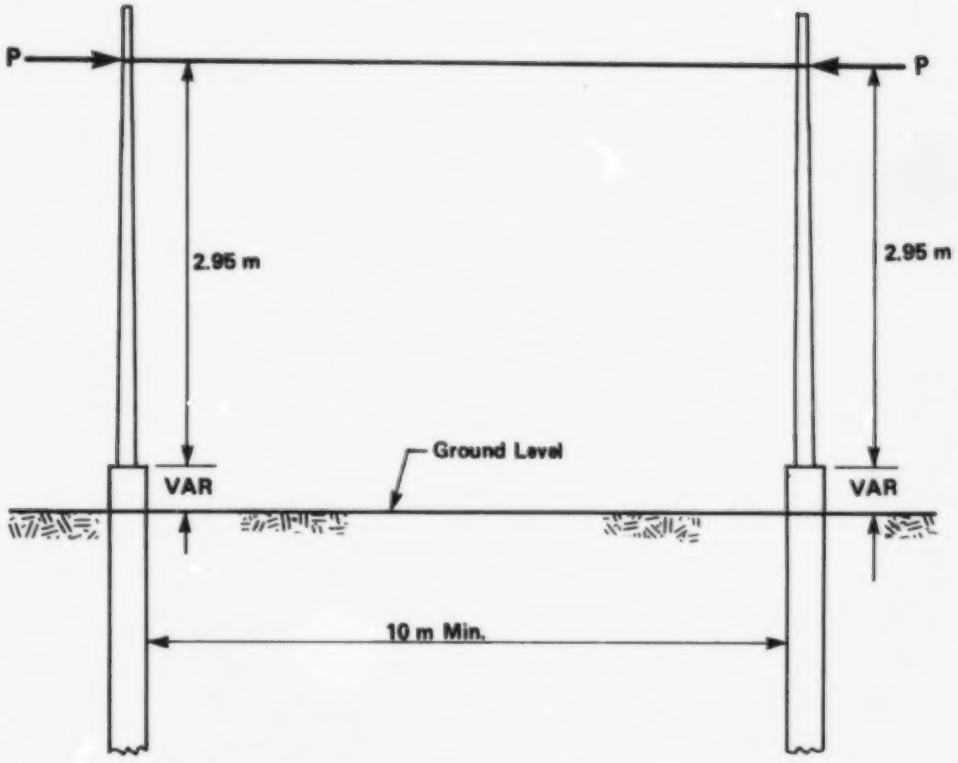

Figure 7/ Typical Installation of Test Mast

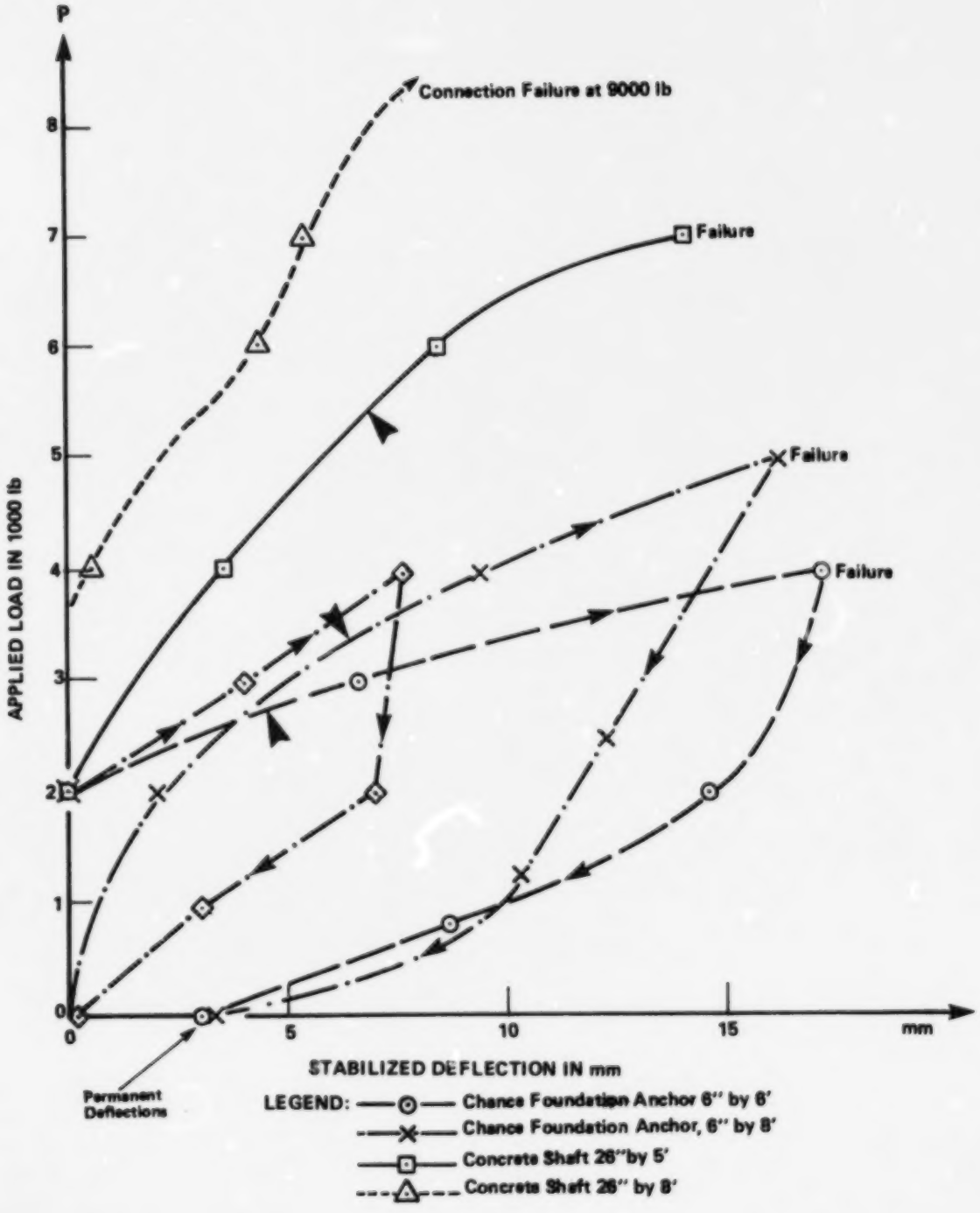

Figure 8/ Ottawa Tests in September 1985, Clay

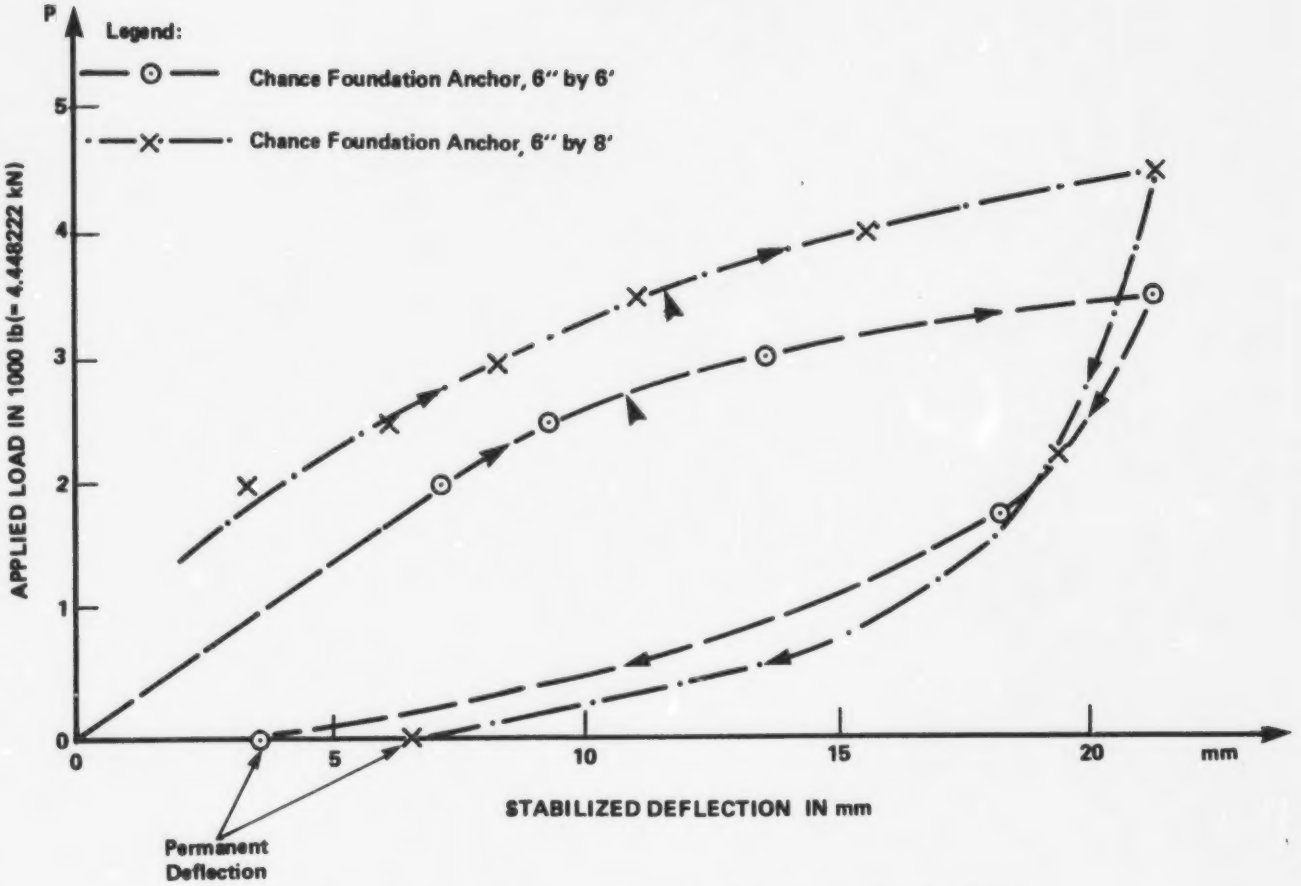

Figure 9/ Repeated Ottawa Tests in the Begining of May, 1986, Clay

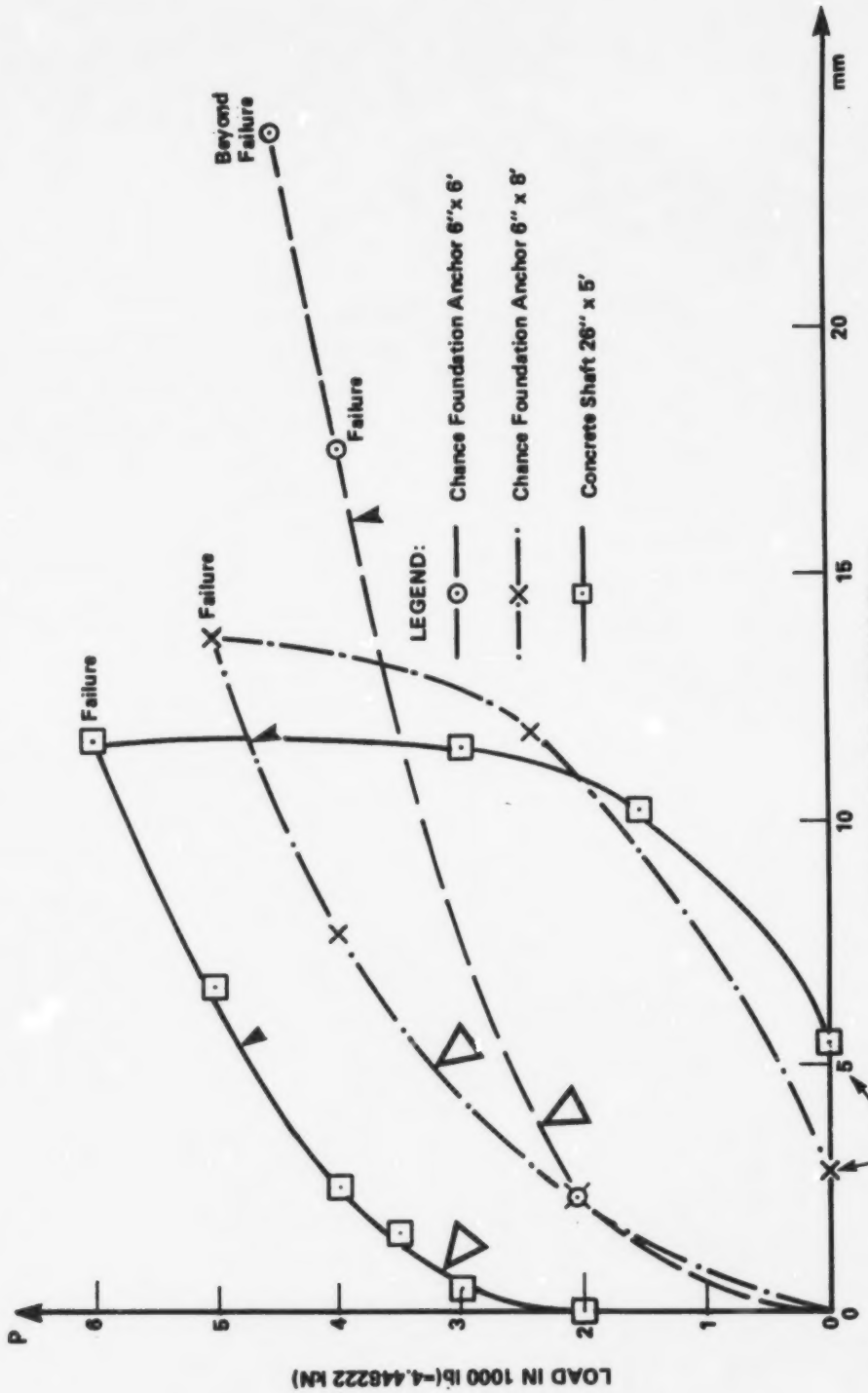

Figure 10/ Hamilton Tests in September 1985, Silt